World Scientific Research Journal Volume 9 Issue 12, 2023
ISSN: 2472-3703 DOI: 10.6911/WSRJ.202312_9(12).0007

Research Progress of Terahertz Coal Level Detection Technology

Tao Chen, Yongbin Guo, Xiangdong Li*, Zhongmin Wang, Mei Chai, Zijiang Yang

Key Laboratory of UWB & THz of Shandong Academy of Sciences, Institute of Automation, Qilu University of Technology (Shandong Academy of Sciences), Jinan, 250014, China

* Corresponding authors: lxd0191@163.com

Abstract

Accurate measurement of coal levels in coal bins is a critical step in the coal production and storage process. Real-time information about changes in coal levels within a closed storage environment can provide a better basis for coal production and scheduling. This study aims to comprehensively and deeply understand the main development status of coal level detection technology and the accuracy of coal bunker detection. To achieve this, we first provide a comprehensive summary of the existing closed coal bunker detection devices and methods. We then systematically analyze the typical structure and principles of terahertz coal-level detection radar. Finally, we evaluate the results of THz coal-level radar detection and discuss the impact of different algorithms on the accuracy of coal-level measurement results. The combination of terahertz radar and advanced algorithms to improve detection accuracy highlights the significant potential of terahertz radar in achieving high-precision coal bunkers detection.

Keywords

THz; Coal-level; Radar; Detection accuracy.

1. INTRODUCTION

During the process of coal production, storage and transportation are typically necessary. The two main forms of storage are stockpile storage and silo storage[1]. Due to economic development, social progress, and more stringent environmental regulations, a growing number of companies are adopting closed-silo coal storage[2].Silo storage coal offers several key advantages [3]. Firstly, it provides good environmental protection performance by completely preventing the diffusion pollution of coal dust [4].

Storing and unloading coal can lead to a significant amount of dust accumulation in the coal bunker[5]. To avoid excessive dust density, it is necessary to maintain a certain level of humidity, which causes coal powder to stick to the bunker walls [6]. The uneven accumulation of coal scale on the bunker walls creates a rough surface that makes it difficult to distinguish between the coal and the bunker walls. Moreover, the coal height in the bunker constantly changes with coal production and transportation[7]. This complex storage environment poses a significant challenge for accurately detecting coal levels in the bunker.

Terahertz radar is a non-destructive detection technology based on the terahertz frequency band[8]. The frequency of the terahertz band is between microwaves and infrared, which has high penetration and resolution and can be used to detect and image a variety of substances and materials[9]. This technology is mainly used in the production and management of coal mines to achieve fast and accurate detection and positioning of coal seams in coal bunkers, thereby improving the utilization of coal bunkers, reducing coal waste, and improving production efficiency. The terahertz radar coal bunker and coal seam detection technology has the advantages of non-contact, non-destructive, high accuracy, and high reliability, and has a broad application prospect in coal production and management[10].

2. COAL BUNKER COAL LEVEL DETECTION DEVICE

Various methods can be used to measure the coal level in a bunker. Depending on whether the measuring instrument makes contact with the coal surface, the coal level depth detection method can be classified as either contact or non-contact measurement method[11]. The pressure method, heavy hammer method, capacitance method, and other instruments are in direct contact with the coal surface during the measurement process, which makes them part of the contact measurement method. On the other hand, the ultrasonic method, laser method, nuclear radiation method, machine vision, and radar-type instruments do not make contact with the coal surface during the measurement process, which classifies them as part of the non-contact measurement method.

2.1. Contact coal bunker level meter

The pressure coal level meter is a device that measures the height of the coal level by weighing the coal stored in the silo[12]. Typically located at the bottom of the silo, it consists of a pressure sensor and a coal-level display[13-15]. The heavy hammer coal level meter is an instrument used for measuring the depth of large or pulverized coal particles in the coal bunker[16, 17]. It comprises a host, a motor, and a controller. The host is installed at the top of the bunker using a heavy hammer detection host and a pulley. The heavy hammer is pulled by the motor via a stainless-steel belt or wire rope, and it is vertically hoisted in the silo through the pulley. The heavy hammer falls freely under the influence of gravity onto the surface of the coal pile or coal bunker, and the coal level height is calculated based on the intensity and time of the energy reflected back[18]. The capacitive coal level meter is made up of a capacitive liquid level sensor and a capacitance detection circuit[19]. Its working principle is based on the fact that the capacitive coal level sensor converts changes in the coal level into changes in capacitance and dielectric constant, which are then used to calculate the material level value[20-22].

2.2. Non-contact coal level meter

Ultrasonic coal level meters typically consist of a detector, a controller, and a display[23]. The sensor receives the reflected signals and converts them into electrical signals, thereby obtaining height information of the coal level[24-26]. The laser coal level meter consists of laser signal transmitters and receivers[27, 28]. By accurately recording the time difference between laser emission and reception, the distance from the laser radar to the target can be determined. The principle of the radioactive coal level meter is to measure the coal level by transmitting energy attenuation when the ray penetrates the coal bunker and its materials[29-31]. The ray receiver is typically installed at the bottom of the coal bunker. As the ray passes through the coal seam of different thicknesses, its strength changes[32]. By detecting the received ray intensity, the height of the object to be measured can be indicated[33, 34]. With the advancement of image recognition technology, computer vision is now being used to detect the coal level in coal bunkers by utilizing an auxiliary light source. The principle of coal level detection in the coal bunker is based on the spot measurement method. The relationship between spot size and coal level is calculated by projection, and then the coal level corresponding to different spots is determined by calibration [35].

3. RADER COAL LEVEL METER

Radar coal level gauge is a non-contact coal level measurement device that utilizes radar technology. It measures the height of coal level by emitting radar signals towards the coal and receiving the signals reflected back from the coal[36-39]. Radar coal level gauges typically have high measurement accuracy and reliability, and can adapt to different coal properties, humidity, viscosity, and other conditions. They are capable of continuous monitoring of coal level, providing real-time information on coal level changes[40-42].

Radar frequency bands can be divided into over-the-horizon radar, microwave radar, millimeter wave radar, terahertz radar, etc. When detecting materials in the coal bunker, over-the-horizon radar is mainly used in short-wave frequency bands, but the measurement distance does not meet the requirements of coal-level detection in the coal bunker[43]. Therefore, over-the-horizon radar is not selected as a detection instrument in the coal bunker coal level detection process.

The principle behind the microwave radar coal level meter is based on emitting an extremely narrow microwave pulse through the antenna radar probe[40]. . This pulse travels through the air at the speed of light and comes into contact with the surface of the medium to be measured, which reflects a portion of the electromagnetic wave. The reflected electromagnetic wave is then received by the antenna in the radar system[44, 45]. The distance from the antenna to the surface of the medium has a positive correlation with the interval between the transmitted and received pulses. Since the propagation speed of the electromagnetic wave is known, the distance from the target can be calculated by determining its time interval [46].

Millimeter wave refers to an electromagnetic wave with a wavelength range of 1-10mm, and its corresponding frequency range is 30GHz-300GHz[4]. Under the same antenna size, the beam of a millimeter wave is much narrower than that of a microwave, so it can distinguish small targets closer to each other or observe the details of targets more clearly[47-49].

Among the various applications of Terahertz waves in industry, Terahertz radar is one of the most important research areas. Terahertz waves refer to electromagnetic waves with frequencies in the range of 0.1~1THz. Compared to existing microwave and millimeter wave technology, Terahertz waves have shorter wavelengths and can achieve larger signal bandwidth and narrower antenna beams, making them ideal for high-resolution target detection[50, 51]. Terahertz radar possesses ultra-wideband characteristics. The large bandwidth enables the radar to achieve fine range resolution, allowing accurate positioning and shape profiling. Ultra-wideband signals can penetrate and propagate through many materials, permitting the detection of objects behind obstacles. Brian Yamauchi used ultra-wideband (UWB) radar to provide obstacle detection capabilities for a portable robot, and validated that UWB radar can effectively penetrate adverse weather including dense fog and detect obstacles undetectable by vision or lidar under the same conditions[52].Fernando Cunha proposed ultra-wideband (UWB) radar as a powerful sensing solution, and validated the performance of this radar in typical coal mining environments, providing higher resolution and greater range in smoke- and dust-filled tunnels[53].

Given these technical characteristics, radar systems based on Terahertz bands are more suitable than traditional microwave and millimeter wave technology for coal level detection in closed silos[54]. This is because the smaller Terahertz wavelength can detect smaller targets more accurately, even in fully enclosed coal bunkers with serious dust[55]. Furthermore, Terahertz radar devices are smaller and their components can be easily placed in a closed coal bunker. As they do not have any movable mechanical parts and are completely isolated from the container volume, they exhibit excellent stability and have low maintenance costs. The measurement of coal level accuracy is vital in the production and transportation of coal, and Terahertz radar's higher bandwidth allows for more accurate detection of coal level in coal bunkers [56].

4. STRUCTURE AND PRINCIPLE OF TERAHERTZ RADAR

Terahertz radar technology, used for level measurement, can be categorized into pulse wave radar and frequency-modulated continuous wave (FMCW) radar, based on the form of the radar signal[57]. The pulse radar system is relatively simple and cost-effective, but when applied to the close-range liquid level measurement, the short pulse round-trip delay makes a direct measurement of the delay challenging, leading to reduced accuracy. FMCW radar, on the other hand, uses linear frequency modulation and fast Fourier transform (FFT) analysis, which reduces the hardware cost requirements of the radar system[58, 59]. In the signal processing phase, by analyzing the frequency domain characteristics of the radar wave, distance parameters of the object target can be obtained, and selecting the appropriate linear bandwidth modulation method can achieve higher distance resolution and more accurate measurement distance. Therefore, for accurate coal level measurement in coal bunkers, FMCW radar is an ideal option, especially as modern industry demands higher accuracy.

4.1. FMCW radar system structure

The diagram in Figure 1 illustrates the basic structure of an FMCW radar system. To measure the distance of a target, the FMCW radar sends a linear frequency modulation pulse[44]. This pulse is generated by a linear frequency modulation source in the radio frequency front end. The frequency modulation source comprises a signal modulator and a voltage-controlled oscillator, with the signal modulator producing the required modulation signal such as a triangular wave or sawtooth wave[41, 60]. The voltage-controlled oscillator, which can be used as the frequency modulator, generates an output signal with a frequency controlled by a slope and periodic ramp signal. A portion of the frequency modulated continuous wave passes through the power divider and is transmitted to the transmitting link. It then passes through the power amplifier, radiating outward via the transmitting antenna. The other part of the mixer sent to the receiving link is used as the local oscillator signal. When the transmitted signal from the transmitting antenna detects the target object, a reflected signal is generated containing information about the target. The reflected signal is received by the receiving antenna, amplified by a low noise amplifier (LNA) and down-converted to generate an intermediate frequency signal. This signal is then sent to the analog-to-digital converter for sampling, and the digital signal processor analyzes the signal to obtain the distance information of the measured target[61].

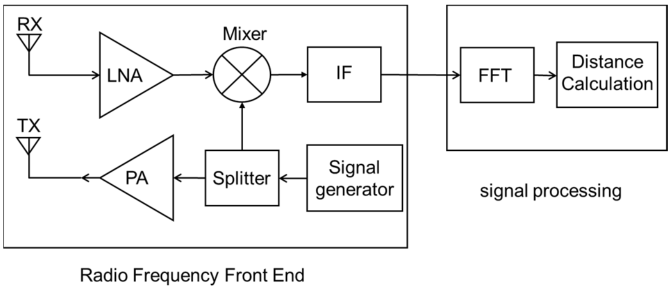

Figure. 1 FMCW radar system structure diagram

4.2. FMCW radar system ranging principle

The figure in Figure 2 shows the waveform of the FMCW radar transmitting and receiving signals on the same time axis.

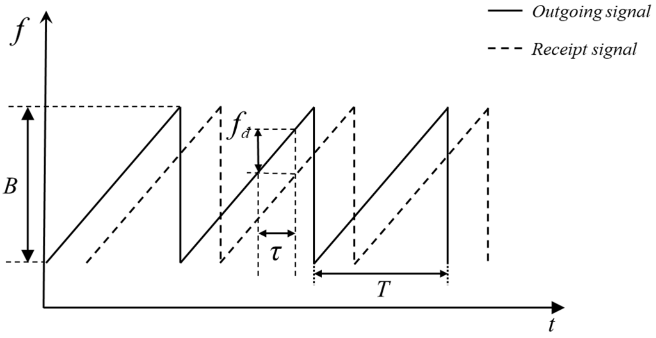

Figure. 2 FMCW signal diagram

The frequency of the frequency-modulated continuous wave changes linearly with time according to the sawtooth wave modulation signal waveform. At any given time t, the frequency of the frequency-modulated continuous wave can be expressed as:

$$f_t = f_0 + kt \tag{1}$$

$$k = \frac{B}{T} \tag{2}$$

The formula given above shows that the frequency of the frequency-modulated continuous wave changes linearly with time. Here, f_0 represents the initial frequency of the frequency-modulated continuous wave, B is the frequency bandwidth of the frequency-modulated continuous wave, τ is the delay between the radar receiving echo signal and the transmitting signal, and T represents the period of the sawtooth wave modulation. The amplitude of the modulated signal remains constant, and the emission frequency changes linearly within a fixed period. As a result, the emitted waveform and the echo waveform are identical. The figure depicted in Figure 2 shows that $f_t(t)$ is the frequency of the transmitted signal at time t, while $f_r(t)$ represents the frequency of the received signal at time t. The mixer multiplies the transmitted signal with the received signal, and the resulting signal is then passed through a low-pass filter to generate a low-frequency signal f_d, also known as the beat frequency signal [44, 60].

According to radar principles, let us assume that the distance between the radar and the target object is R, and the electromagnetic wave propagation velocity is c=3×108 m/s. and the electromagnetic wave propagation velocity is t_0, and receives the echo signal at time $t_0 + \tau$. Then the distance of the signal propagation is 2R, which can be calculated using the following relationship

$$\tau = \frac{2R}{c} \tag{3}$$

From the above equation, $\mathrm{f_d}$ is the frequency difference between the transmitted signal and the echo signal

$$f_d = k\tau \tag{4}$$

Combining the above equations, the frequency difference f_d between the transmitted signal and the received signal is:

$$f_d = 2R\frac{B}{cT} \tag{5}$$

The distance R between the radar and the target object is:

$$R = \frac{cT}{2B} f_d \tag{6}$$

From the above, it can be observed that the radar detection range R is dependent on the sawtooth sweep period T, the sweep bandwidth B, and the frequency difference between the transmitted signal and the received signal. In a radar system, the sweep bandwidth and the sweep period are usually known values[62, 63]. Hence, if the frequency difference can be determined, the distance R between the radar and the target can be calculated. During the signal processing stage, the frequency difference signal is sampled and subjected to Fourier transformation. At this point, the peak value in the signal spectrum can be determined, and the value corresponding to the peak frequency is f_d.

5. ALGORITHM FOR IMPROVING RANGING ACCURACY OF FMCW RADAR

5.1. DFT zero-padding method

Suppose that the sequence $x(n)$ has N sampling points, if it is zero-padded to a length of N0, then the new sequence $x_0(n)$ is

$$x_0(n) = \begin{cases} e^{j2\pi t_d\left(B\frac{n}{N}+f_0\right)}, 0 \le n \le N \\ 0, N \le n \le N_0 \end{cases} \tag{7}$$

$X_0(k)$ is obtained by N0 point discrete Fourier transform of $x_0(n)$. If N0=AN, the relationship between $X_0(k)$ and $x(n)$ is

$$X_0(k) = \sum_{n=0}^{N-1} x(n) e^{-j2\pi\frac{n}{AN}}, 0 \le k \le AN \tag{8}$$

$$X_0(\mathrm{Ak}) = X(k) \tag{9}$$

$X(k)$ can be obtained by sampling the spectrum of $X_0(k)$ at A points. As a result, the spectral lines of $X_0(k)$ around A point become denser than the adjacent spectral lines of $X(k)$ at the same distance, which increases the spectral line density and enhances the ranging accuracy[64, 65]. However, the spectral line density of the zero-padding method is directly proportional to the number of zero-padding [66, 67]. Increasing the number of zero-padding will increase the computational burden on the backend of digital signal processing, resulting in significant time loss during data processing.

5.2. Zoom—FFT

Although the zero-padding method in the time domain can improve the accuracy of frequency measurement, it increases the amount of calculation in the back end of digital signal processing. In the spectrum analysis of FMCW radar, the goal is to identify the maximum spectrum peak position of the beat frequency signal, and the other spectrum components are not necessarily refined. The ZFFT method refines the local part of the spectrum to improve frequency measurement accuracy while increasing the calculation amount[68, 69].

Assuming the signal $x(t)$ is sampled at a rate of f_s and has a sampling sequence $x(n)$, a distance dimension FFT is performed on the sequence with N points to obtain the signal frequency f_{peak} corresponding to the spectrum peak. The center frequency f_{peak}, the starting frequency f_1, and the end frequency $f_2 + B$ are shifted to the zero-point, and then a low-pass filter is applied to filter out high-frequency components that are not relevant and prevent spectrum aliasing after sampling. The filtered signal is resampled with a refinement factor D, resulting in N0 signal points. Zero is added to make the number of points N before extraction, and N-point FFT is performed to improve the accuracy of the ranging results.[70-72].

5.3. Chirp—Z transform

To address the contradiction of the simple FFT method, the Chirp-z transform (CZT) can be utilized to enhance the local sampling resolution without increasing the computational complexity of signal processing. The CZT method is a spectrum calculation technique that employs spiral sampling, enabling the acquisition of a high-precision spectrum with fewer sampling points in the frequency band of interest [73].

When measuring the coal level in the coal bunker, typically only a certain section of the entire spectrum of the beat frequency signal is of interest[74, 75]. The CZT algorithm is capable of sampling at non-unit and non-equal interval points, and then refining the spectrum accordingly. The CZT algorithm operates based on the following fundamental principle[65, 76, 77].

The sequence $x(n)(0 \leq n \leq N-1)$, its Z transform (10) is shown

$$X(z_k) = \sum_{n=0}^{N-1} x(n) z^{-n} \tag{10}$$

A Sampling at equal angles along a helix in the z-plane, the sample points for Z are shown as.

$$z_k = AW^{-k}, k \in [0, M-1] \tag{11}$$

N is the number of sampling points near the selected frequency, A and W can be expressed as:

$$A = A_0 e^{j\theta_0} \tag{12}$$

$$W = W_0 e^{-j\varphi_0} \tag{13}$$

Bring (12) and (13) into (11) to obtain:

$$z_k = A_0 W_0^{-k} e^{j(\theta_0 + k\varphi_0)} \tag{14}$$

In equation (14), A_0 represents the length of the vector radius of the initial sampling point, θ_0 represents the phase angle of the initial sampling point,, φ_0 represents the angle difference between two adjacent sampling points, and W0 represents the elongation of the spiral.

When M = N, A0 = 1, W0 = 1, $\varphi_0 = 2\pi/N$, the calculation formula of CZT is as follows:

$$X(z_k) = \sum_{n=0}^{N-1} x(n) z_k^{-n} = \sum_{n=0}^{N-1} x(n)\, A^{-n} W^{nk}, 0 \leq k \leq M-1 \tag{15}$$

Using the Brustein equation:

$$nk = \frac{1}{2}(n^2 + k^2 - (k-n)^2) \tag{16}$$

Bring (16) into (15) to obtain:

$$X(z_k) = \sum_{n=0}^{N-1} x(n)A^{-n}W^{\frac{1}{2}[n^2+k^2-(k-n)^2]} = W^{\frac{k^2}{2}} \sum_{n=0}^{N-1} \left[x(n)A^{-n}W^{\frac{n^2}{2}}\right] W^{\frac{-(k-n)^2}{2}} \tag{17}$$

Let

$$g(n) = x(n)A^{-n}W^{\frac{n^2}{2}} \ , \ \ n = 0,1,\cdots N-1 \tag{18}$$

$$h(n) = W^{-\frac{n^2}{2}} \tag{19}$$

Then (17) can be rewritten as:

$$X(z_k) = W^{\frac{k^2}{2}} \sum_{n=0}^{N-1} g(n)h(k-n) = W^{\frac{k^2}{2}}[g(k) * h(k)]\,, k = 0,1,\cdots M-1 \tag{20}$$

5.4. Phase estimation algorithm

Accurate estimation of the beat frequency and phase is crucial for achieving precise distance measurement because the frequency and phase are proportional to the distance[57, 65, 78-80]. However, achieving micron-level accuracy requires a very wide bandwidth, which is difficult to achieve in coal bunker coal level measuring instruments. To address this challenge, a combination of frequency and phase estimation can be used to improve frequency accuracy detection[49, 66, 81-85]. Specifically, the phase change of FMCW terahertz radar can be calculated using formula (24).

$$\phi = \frac{4\pi R}{\lambda} \tag{23}$$

The algorithm leverages phase information to partition the range from the radar to the target into n clear range units based on the non-fuzzy range order. The length of each ranging unit is $\lambda_{start}/2$. To determine the distance unit of the target, the frequency estimation provides a rough estimation of the target distance (Rcoarse) using formula (24). The initial phase of the IF signal is equivalent to the phase difference between Tx and Rx, and the time delay between Tx and Rx chirps is stored in the IF value. Therefore, the precise estimation of the target range (Rphase) can be obtained from IF using formula (25) within the determined range unit. The final estimated value of the target distance is calculated using equation (26).

$$R_{coarse} = f_b \frac{cT}{2B} \tag{24}$$

$$R_{phase} = \frac{\varphi_{IF}\lambda_{start}}{4\pi} \tag{25}$$

$$R_{abs} = R_{coarse} + R_{phase} \tag{26}$$

The frequency estimation is used to determine the rough position of the target, followed by the phase estimation method to accurately determine the position of the target. This approach has been highly effective in detecting the coal level of the coal bunker, enabling rapid and accurate detection.

6. CONCLUSION

This paper provides an overview of the complex environment in a coal bin and typical closed coal bin detection devices and methods. The focus is on the analysis and processing algorithms for the beat frequency signal used in Terahertz radar measurement, which enables higher detection accuracy. The precise detection method based on Terahertz radar holds significant potential and advantages for coal seam level detection. Compared to other detection devices, the Terahertz radar-based method exhibits strong anti-jamming capabilities, high detection accuracy, superior performance, and ease of installation. Furthermore, with the continuous upgrade of digital signal processing backend equipment and the development of processing algorithms, coal-level detection technology based on Terahertz radar is expected to achieve further breakthroughs and advancements.

ACKNOWLEDGMENTS

Ethical Approval not applicable

Competing interests The authors declare no competing interests.

Authors' contributions Tao Chen and Yongbin guo: wrote the main manuscript text .Xiangdong Li and Zhongmin Wang: Supervision. Mei Chai: Investigation. Zijiang Yang: Methodology.

Funding This work was supported by Natural Science Foundation of Shandong Province(No. ZR2022MF276), Major innovation fund of Qilu University of Technology (Shandong Academy of Science)(No.2022JBZ02-02)and National Foreign Expert Program (High end Foreign Expert Introduction Program)G2022024005L

Availability of data and materials All data created and analyzed during this study are included in this published letter.

REFERENCES

[1] K.H. Voss New stowing material and raw coal bunkers in the coal mining industry, Glueckauf123, (10), 1987.

[2] H. An, X. Wang, X. Fang, Z. Liu.and C. Liang Wall normal stress characteristics in an experimental coal silo, Powder Technology, 377, 657-665, 2021.

[3] J. Carson.and D. Goodwill The design of large coal silos for safety, reliability and economy, Bulk Solids Handl., 4, (1), 1984.

[4] G. Brooker, R. Hennessey, C. Lobsey, M. Bishop.and E. Widzyk-Capehart Seeing through dust and water vapor: Millimeter wave radar sensors for mining applications, Journal of Field Robotics, 24, (7), 527-557, 2007.

[5] Z. Wang, S. Shang, L. Gao, L. Sun, J. Lu, D. Xue, G. Zhang, J. Lu, Z. Huang, Z. He, J. Liu, G. Yuan, H. Zhang, H. Ding, Y. Zhu, C. Chen, L. Qi, L. Chu, Q. Zhao, Y. Yu, L. Dong.and L. Zhang Research development and application of coal bunker cleaning robot, Meitan Kexue Jishu/Coal Science and Technology (Peking), 50, (9), 215-221, 2022.

[6] Z. Xiu, W. Nie, J. Yan, D. Chen, P. Cai, Q. Liu, T. Du.and B. Yang Numerical simulation study on dust pollution characteristics and optimal dust control air flow rates during coal mine production, Journal of Cleaner Production, 248, 119197, 2020.

[7] X. Yuanfang, J. Yuanyuan.and L. Zhe Detection of coal level in underground coal bins using an improved edge detection algorithm, Journal of Multimedia, 9, (6), 796, 2014.

[8] F. Sizov.and A. Rogalski THz detectors, Progress in quantum electronics, 34, (5), 278-347, 2010.

[9] Y.-P. Zhang, T. Li-Bin, L. Yu-Fei, K.S. Teng, W. Gang, H. Wei-Da.and H. Fu-Zhong The research progress and application of novel terahertz detectors, Journal of Infrared Millimeter Waves, 39, (2), 191, 2020.

[10] J. Deng, J. Ornik, K. Zhao, E. Ding, M. Koch.and E.J.O.E. Castro-Camus Recognition of coal from other minerals in powder form using terahertz spectroscopy, 28, (21), 30943-30951, 2020.

[11] X. Yuan-fang.and Z. Meng-ran Research on Coal Level Detecting System of Mine Coal Bunker, Coal Mine Machinery, 34, (05), 13-15, 2013.

[12] D. Sear, W. Damon, D. Booker.and D. Anderson A load cell based continuous recording bedload trap, Earth Surface Processes Landforms, 25, (6), 659-672, 2000.

[13] P. Chalupa, M. Vlacil.and J. NovakA Liquid Level Monitoring System for a Remote Reservoir, in Editor (Ed.)^(Eds.): Book A Liquid Level Monitoring System for a Remote Reservoir (2019, edn.), pp. 80-85.

[14] S. Qingfang, K. Yali, S. Kai.and C. Bing Application of sensors in China coal preparation plant, Industry and Mine Automation, 40, (02), 26-29, 2014.

[15] M. Su-ping.and K. Zi-ming Study on coal level auto monitoring and control system of deep and small diameter coal bunker, Coal Science and Technology, (06), 31-34, 2001.

[16] [Y.-F. Xin.and M.-R. Zhou Research on coal level detecting system of mine coal bunker, Meikuang Jixie, 34, (5), 13-15, 2013.

[17] L. Zhiqiang, W. Baihai.and W. Xiaoji Application and research of image recognition technique in weighting hammer level indicator, Fluid Power Transmission Control, 35, (4), 36-39, 2009.

[18] [X. Zi-kang Application of Weighting Hammer Level Indicator in Guixi Smelter Copper Engineering, (04), 65-68, 2010.

[19] K. Matsumoto, M. Sobue, K. Asamoto, Y. Nishimura, S. Abe.and T. Numazawa Capacitive level meter for liquid hydrogen, Cryogenics, 51, (2), 114-115, 2011.

[20] S. Kv.and P. MohantyImplementation of Intelligent Auto Ranging Functionality to Capacitive Level Sensor, in Editor (Ed.)^(Eds.): Book Implementation of Intelligent Auto Ranging Functionality to Capacitive Level Sensor (IEEe, 2018, edn.), pp. 1-6.

[21] N. Wen-feng, X. Zhi-peng, W. Zhong-bin.and H. Ke-wei New Capacitive Coal Level Automatic Monitoring System Design, Coal Mine Machinery, (06), 126-128, 2008.

[22] W. Zong, X. Deng.and Y. Zhao Research on powder coal position measurement with capacitive sensor, Zhongguo Kuangye Daxue Xuebao, 28, 1999.

[23] J.Y. Cho.and M.H. Kang Design of a Ultrasonic Oil Level Meter Using a FPGA, Journal of the Institute of Electronics Information Engineers, 49, (11), 167-174, 2012.

[24] P. Olmos Extending the accuracy of ultrasonic level meters, Measurement Science Technology, 13, (4), 598, 2002.

[25] A. Petrauskas.and P. Razutis Investigation of echolocational ultrasonic methods by increasing accuracy in level measurements, Ultragarsas/Ultrasound, 41, (4), 18-21, 2001.

[26] R. Reeve Mounting of sensors in coal hoppers and bunkers, Ultrasonics, 4, (2), 96, 1966.

[27] Y. Depeng, W. Jiping, Z. Jinxing, C. Xiaoxue.and R. Huijun Monitoring slope deformation using a 3-D laser image scanning system: a case study, Mining Science Technology, 20, (6), 898-903, 2010.

[28] C. Fengyun.and C. Xudong Design of detection system for non-contact laser level, Measurement Technique, 3, 13-15, 2008.

[29] J. Gu, J. Liu, J. Xue.and D. XingPrinciples and Applications of Continuous Level Gauges in Level Monitoring of Solid Particles, in Editor (Ed.)^(Eds.): Book Principles and Applications of Continuous Level Gauges in Level Monitoring of Solid Particles (IOP Publishing, 2018, edn.), pp. 022050.

[30] J. Sun.and J. Jiang Laser triangulation measurement of the level in a coal silo, Mining Science Technology, 21, (6), 881-884, 2011.

[31] L.-g. Wang, Z.-k. Zhang, Y.-l. Lu, H.-b. Yang, S.-q. Yang, S. Jian.and J.-y. Zhang Combined ANN prediction model for failure depth of coal seam floors, Mining Science Technology, 19, (5), 684-688, 2009.

[32] H.F. Kaiser A Completely Portable Radioactivity Meter Requiring No High Voltage Battery, Review of Scientific Instruments, 10, (7), 218-219, 1939.

[33] P.V. Brady, B.W. Arnold, G.A. Freeze, P.N. Swift, S.J. Bauer, J.L. Kanney, R.P. Rechard.and J.S. Stein Deep borehole disposal of high-level radioactive waste, Sandia Report SAND-, Sandia National Laboratories, Albuquerque, New Mexico, 2009.

[34] C. Qunying.and S. Dongfeng Measurement method for level of coalfly ash based on nuclear radiation field theory, China Patent.

[35] Q. Tiezhu, C. Xin.and S. Ruiping Study on new adaptive calibration technique of coal level detection in coal bin with binocular vision, Chinese Journal of Scientific Instrument, 34, (07), 73-78, 2013.

[36] W.A. Ahmad, M. Kucharski, H.J. Ng.and D. KissingerD-Band FMCW Radar with sub-cm Range Resolution based on a BiCMOS mm Wave IC, in Editor (Ed.)^(Eds.): Book D-Band FMCW Radar with sub-cm Range Resolution based on a BiCMOS mm Wave IC (IEEE, 2022, edn.), pp. 533-536.

[37] W.A. Ahmad.and X. Yi How Will Radar Be Integrated Into Daily Life?: mm-Wave Radar Architectures for Modern Daily Life Applications, IEEE Microwave Magazine, 23, (5), 30-43, 2022.

[38] J.-M. Kim, Z.-S. Lim, J.-C. Chun.and T.-S. Kim Correlation algorithm for high-precision measurement in FM-CW radar level meters, IEICE transactions on communications, 84, (8), 2326-2329, 2001.

[39] J. OttoRadar applications in level measurement, distance measurement and nondestructive material testing, in Editor (Ed.)^(Eds.): Book Radar applications in level measurement, distance measurement and nondestructive material testing (IEEE, 1997, edn.), pp. 1113-1121.

[40] X.H. ChengRadar Level Meter Measurement in the Storage Silo, in Editor (Ed.)^(Eds.): Book Radar Level Meter Measurement in the Storage Silo (Trans Tech Publ, 2012, edn.), pp. 6600-6603.

[41] C. Li, W. Chen, G. Liu, R. Yan, H. Xu.and Y. Qi A noncontact FMCW radar sensor for displacement measurement in structural health monitoring, Sensors, 15, (4), 7412-7433, 2015.

[42] S. Pisa, E. Pittella.and E. Piuzzi A survey of radar systems for medical applications, IEEE Aerospace Electronic Systems Magazine, 31, (11), 64-81, 2016.

[43] Z. Luo, Z. He, X. Chen.and K. Lu Target location and height estimation via multipath signal and 2D array for sky-wave over-the-horizon radar, IEEE Transactions on Aerospace Electronic Systems, 52, (2), 617-631, 2016.

[44] J. Chun, T. Kim, J. Kim, Z. Lim.and W. ParkSpectrum correlation of beat signals in the FM-CW radar level meter and application for precise distance measurement, in Editor (Ed.)^(Eds.): Book Spectrum correlation of beat signals in the FM-CW radar level meter and application for precise distance measurement (IEEE, 2001, edn.), pp. 2251-2254.

[45] M. VogtRadar sensors (24 and 80 GHz range) for level measurement in industrial processes, in Editor (Ed.)^(Eds.): Book Radar sensors (24 and 80 GHz range) for level measurement in industrial processes (IEEE, 2018, edn.), pp. 1-4.

[46] M. Vogt, M. Gerding.and V. FortoulAn optimized radar system for tank level measurement in dispersive bypass pipes, in Editor (Ed.)^(Eds.): Book An optimized radar system for tank level measurement in dispersive bypass pipes (IEEE, 2015, edn.), pp. 178-181.

[47] G.M. Brooker, S. Scheding, M.V. Bishop.and R.C. Hennessy Development and application of millimeter wave radar sensors for underground mining, IEEE Sensors journal, 5, (6), 1270-1280, 2005.

[48] S. Jeon, J. Mun, S. Lee, K. Sim.and S. Kim Design and manufacture of horn lens antennas of 80 GHz MM wave FMCW radar for cryogenic fluids level measurement, Progress in Superconductivity Cryogenics, 24, (1), 29-33, 2022.

[49] M. Pauli, B. Göttel, S. Scherr, A. Bhutani, S. Ayhan, W. Winkler.and T. Zwick Miniaturized millimeter-wave radar sensor for high-accuracy applications, IEEE Transactions on Microwave Theory Techniques, 65, (5), 1707-1715, 2017.

[50] C. Am Weg, W. von Spiegel, R. Henneberger, R. Zimmermann, T. Loeffler.and H.G. Roskos Fast active THz cameras with ranging capabilities, Journal of Infrared, Millimeter,Terahertz Waves, 30, 1281-1296, 2009.

[51] F. Friederich, K.H. May, B. Baccouche, C. Matheis, M. Bauer, J. Jonuscheit, M. Moor, D. Denman, J. Bramble.and N. SavageTerahertz radome inspection, in Editor (Ed.)^(Eds.): Book Terahertz radome inspection (MDPI, 2018, edn.), pp. 1.

[52] B. YamauchiAll-weather perception for man-portable robots using ultra-wideband radar, in Editor (Ed.)^(Eds.): Book All-weather perception for man-portable robots using ultra-wideband radar (IEEE, 2010, edn.), pp. 3610-3615.

[53] F. Cunha.and K. Youcef-ToumiUltra-wideband radar for robust inspection drone in underground coal mines, in Editor (Ed.)^(Eds.): Book Ultra-wideband radar for robust inspection drone in underground coal mines (IEEE, 2018, edn.), pp. 86-92.

[54] Y. Jiang, B. Deng, H. Wang, Y. Qin.and K. Liu An effective nonlinear phase compensation method for FMCW terahertz radar, IEEE Photonics Technology Letters, 28, (15), 1684-1687, 2016.

[55] Y. Li, W. Hu, X. Zhang, Y. Zhao, J. Ni.and L.P. Ligthart A non-linear correction method for terahertz LFMCW radar, IEEE Access, 8, 102784-102794, 2020.

[56] T.M. Wong, M. Kahl, P. Haring Bolívar.and A. Kolb Computational image enhancement for frequency modulated continuous wave (FMCW) THz image, Journal of Infrared, Millimeter Terahertz Waves, 40, 775-800, 2019.

[57] Q. GuoqingDigital signal processing in FMCW radar marine tank gauging system, in Editor (Ed.)^(Eds.): Book Digital signal processing in FMCW radar marine tank gauging system (IEEE, 1996, edn.), pp. 7-10.

[58] A.G. StoveLinear FMCW radar techniques, in Editor (Ed.)^(Eds.): Book Linear FMCW radar techniques (IET, 1992, edn.), pp. 343-350.

[59] M. Vossiek, T.v. Kerssenbrock.and P. HeideSignal processing methods for millimetrewave fmcw radar with high distance and doppler resolution, in Editor (Ed.)^(Eds.): Book Signal processing methods for millimetrewave fmcw radar with high distance and doppler resolution (IEEE, 1997, edn.), pp. 1127-1132.

[60] S. Lee, B.-H. Lee, J.-E. Lee.and S.-C. Kim Statistical characteristic-based road structure recognition in automotive FMCW radar systems, IEEE Transactions on Intelligent Transportation Systems, 20, (7), 2418-2429, 2018.

[61] J. Zhang.and R. BaiA level measurement system of the FMCW radar based on Virtual instruments, in Editor (Ed.)^(Eds.): Book A level measurement system of the FMCW radar based on Virtual instruments (Trans Tech Publ, 2011, edn.), pp. 337-341.

[62] H.-H. Ko, K.-W. Cheng.and H.-J. SuRange resolution improvement for FMCW radars, in Editor (Ed.)^(Eds.): Book Range resolution improvement for FMCW radars (IEEE, 2008, edn.), pp. 352-355

[63] T. Little Effective solids level measurement with radar, Zkg International, 57, 48-55, 2004.

[64] Q. GuoqingHigh accuracy range estimation of FMCW level radar based on the phase of the zero-padded FFT, in Editor (Ed.)^(Eds.): Book High accuracy range estimation of FMCW level radar based on the phase of the zero-padded FFT (IEEE, 2004, edn.), pp. 2078-2081.

[65] S. Scherr, S. Ayhan, M. Pauli.and T. ZwickAccuracy limits of a K-band FMCW radar with phase evaluation, in Editor (Ed.)^(Eds.): Book Accuracy limits of a K-band FMCW radar with phase evaluation (IEEE, 2012, edn.), pp. 246-249.

[66] Q. Guoqing, L. Xueling.and T. YanyanRange estimation accuracy analysis of the FMCW level radar, in Editor (Ed.)^(Eds.): Book Range estimation accuracy analysis of the FMCW level radar (IEEE, 2006, edn.), pp.

[67] P.T. Nguyen, V.T. Nhat.and C.P. HuynhA high-resolution short-range X-band FMCW radar system for ranging applications, in Editor (Ed.)^(Eds.): Book A high-resolution short-range X-band FMCW radar system for ranging applications (IEEE, 2014, edn.), pp. 675-680.

[68] B. Al-Qudsi, N. Joram, A. Strobel.and F. EllingerZoom FFT for precise spectrum calculation in FMCW radar using FPGA, in Editor (Ed.)^(Eds.): Book Zoom FFT for precise spectrum calculation in FMCW radar using FPGA (IEEE, 2013, edn.), pp. 337-340.

[69] N. Fernandes, R. Chaudhari.and A. KhandareFPGA Implementation of GPR Signal Analysis using Modified Zoom FFT, in Editor (Ed.)^(Eds.): Book FPGA Implementation of GPR Signal Analysis using Modified Zoom FFT (IEEE, 2019, edn.), pp. 1-6.

[70] E. Hoyer.and R. StorkThe zoom FFT using complex modulation, in Editor (Ed.)^(Eds.): Book The zoom FFT using complex modulation (IEEE, 1977, edn.), pp. 78-81.

[71] Z. Ming-xuan, G. Jiao-bo, M. He-min, F. Zhe, Z. Ya-wei.and L. Jun-na Zoom-FFT based on Fourier transform spectroscopy, Journal of Applied Optics, 34, (3), 452-456, 2013.

[72] D. Pei, S. Yang, H. Yang, Q. Wang.and M. LiHigh efficient and real-time realization of Zoom FFT based on FPGA, in Editor (Ed.)^(Eds.): Book High efficient and real-time realization of Zoom FFT based on FPGA (IEEE, 2010, edn.), pp. V2-669-V662-673.

[73] K. Babaeian, M. Modarres-Hashemi, S.J. Zahabi.and M.M. NaahshA CZT-Based Algorithm for Improving Multi-Target Ranging in FMCW Radar, in Editor (Ed.)^(Eds.): Book A CZT-Based Algorithm for Improving Multi-Target Ranging in FMCW Radar (IEEE, 2019, edn.), pp. 1465-1469.

[74] T. Huang, C. Zhang, D. Lu, Q. Zeng, W. Fu.and Y. Yan Improving FMCW GPR Precision through the CZT Algorithm for Pavement Thickness Measurements, Electronics, 11, (21), 3524, 2022.

[75] S. Scherr, S. Ayhan, H. Gulan, M. Pauli.and T. Zwick61 GHz ISM band FMCW radar for applications requiring high accuracy, in Editor (Ed.)^(Eds.): Book 61 GHz ISM band FMCW radar for applications requiring high accuracy (IEEE, 2014, edn.), pp. 1118-1120.

[76] Y. Wang, Z. Xiao.and J. Xu A novel threshold detection method for fmcw radar, IET International Radar Conference 2015, 2015.

[77] C. Xianzhong, M. Liangliang.and H. QingwenThe improved phase-difference algorithm of 24GHz FMCW radar for fast level tracing of bulk solid material, in Editor (Ed.)^(Eds.): Book The improved

phase-difference algorithm of 24GHz FMCW radar for fast level tracing of bulk solid material (IEEE, 2010, edn.), pp. V3-181-V183-184.

[78] S. Scherr, S. Ayhan, B. Fischbach, A. Bhutani, M. Pauli.and T. Zwick An efficient frequency and phase estimation algorithm with CRB performance for FMCW radar applications, IEEE Transactions on Instrumentation Measurement, 64, (7), 1868-1875, 2014.

[79] P. Pahl, T. Kayser, M. Pauli.and T. ZwickEvaluation of a high accuracy range detection algorithm for FMCW/phase radar systems, in Editor (Ed.)^(Eds.): Book Evaluation of a high accuracy range detection algorithm for FMCW/phase radar systems (IEEE, 2010, edn.), pp. 160-163.

[80] S. Ayhan, S. Scherr, M. Pauli.and T. ZwickFMCW radar in oil-filled waveguides for range detection in hydraulic cylinders, in Editor (Ed.)^(Eds.): Book FMCW radar in oil-filled waveguides for range detection in hydraulic cylinders (IEEE, 2012, edn.), pp. 63-66.

[81] A. Pramudita, F.Y. Suratman, D. Arseno.and E. AliFMCW radar post processing method for small displacement detection, in Editor (Ed.)^(Eds.): Book FMCW radar post processing method for small displacement detection (IEEE, 2018, edn.), pp. 1-5.

[82] A. Chaudhari, S. Prabhu.and R. PintoFrequency estimator to improve short range accuracy in FMCW radar, in Editor (Ed.)^(Eds.): Book Frequency estimator to improve short range accuracy in FMCW radar (IEEE, 2015, edn.), pp. 640-644.

[83] Q. Guoqing.and J. XinleImprovement of measurement accuracy of FMCW level radar, in Editor (Ed.)^(Eds.): Book Improvement of measurement accuracy of FMCW level radar (IEEE, 2001, edn.), pp. 567-570.

[84] S. Scherr, B. Göttel, S. Ayhan, A. Bhutani, M. Pauli, W. Winkler, J.C. Scheytt.and T. ZwickMiniaturized 122 GHz ISM band FMCW radar with micrometer accuracy, in Editor (Ed.)^(Eds.): Book Miniaturized 122 GHz ISM band FMCW radar with micrometer accuracy (IEEE, 2015, edn.), pp. 277-280.

[85] A. Bhutani, S. Marahrens, M. Gehringer, B. Göttel, M. Pauli.and T. Zwick The role of millimeter-waves in the distance measurement accuracy of an FMCW radar sensor, Sensors, 19, (18), 3938, 2019.